

Achieving Unbiased Multi-Instance Learning via Balanced Fine-Grained Positive-Unlabeled Learning

LIN-HAN JIA, National Key Laboratory for Novel Software Technology, Nanjing University, China

LAN-ZHE GUO, National Key Laboratory for Novel Software Technology, Nanjing University, China

ZHI ZHOU, National Key Laboratory for Novel Software Technology, Nanjing University, China

SI-YU HAN, National Key Laboratory for Novel Software Technology, Nanjing University, China

ZI-WEN LI, Didi Chuxing, China

YU-FENG LI, National Key Laboratory for Novel Software Technology, Nanjing University, China

In real-world applications, it is often challenging to detect anomalous samples when the anomalous information they contain is extremely limited. In such cases, both macro-level and micro-level detection using multi-instance learning (MIL) encounter significant difficulties. The former struggles because normal and anomalous samples are highly similar and hard to distinguish at the macro level, while the latter is limited by the lack of labels at the micro level. In MIL, micro-level labels are inferred from macro-level labels, which can lead to severe bias. Moreover, the more imbalanced the distribution between normal and anomalous samples, the more pronounced these limitations become. In this study, we observe that the MIL problem can be elegantly transformed into a fine-grained Positive-Unlabeled (PU) learning problem. This transformation allows us to address the imbalance issue in an unbiased manner using a micro-level balancing mechanism. To this end, we propose a novel framework—Balanced Fine-Grained Positive-Unlabeled (BFGPU)—based on rigorous theoretical foundations to address the challenges above. Extensive experiments on both public and real-world datasets demonstrate the effectiveness of BFGPU, which outperforms existing methods, even in extreme scenarios where both macro and micro-level distributions are highly imbalanced. The code is open-sourced at <https://github.com/BFGPU/BFGPU>.

Additional Key Words and Phrases: Positive-Unlabeled Learning, Weakly Supervised Learning

ACM Reference Format:

Lin-Han Jia, Lan-Zhe Guo, Zhi Zhou, Si-Yu Han, Zi-Wen Li, and Yu-Feng Li. 2025. Achieving Unbiased Multi-Instance Learning via Balanced Fine-Grained Positive-Unlabeled Learning. 1, 1 (June 2025), 21 pages. <https://doi.org/10.1145/nnnnnnnn.nnnnnnn>

1 Introduction

In real-world applications, there is a strong demand for effective detection of anomalous samples, such as in quality inspection, risk control, and fault diagnosis [11, 23, 35]. Ideally, anomalous samples exhibit significant and easily distinguishable differences from normal samples, making them readily separable based on features or representations.

Authors' Contact Information: Lin-Han Jia, jialh@lamda.nju.edu.cn, National Key Laboratory for Novel Software Technology, Nanjing University, Nanjing, China; Lan-Zhe Guo, guolz@lamda.nju.edu.cn, National Key Laboratory for Novel Software Technology, Nanjing University, Nanjing, China; Zhi Zhou, zhouz@lamda.nju.edu.cn, National Key Laboratory for Novel Software Technology, Nanjing University, Nanjing, China; Si-Yu Han, hansy@lamda.nju.edu.cn, National Key Laboratory for Novel Software Technology, Nanjing University, Nanjing, China; Zi-Wen Li, liziwen@didiglobal.com, Didi Chuxing, Beijing, China; Yu-Feng Li, liyf@lamda.nju.edu.cn, National Key Laboratory for Novel Software Technology, Nanjing University, Nanjing, China.

Permission to make digital or hard copies of all or part of this work for personal or classroom use is granted without fee provided that copies are not made or distributed for profit or commercial advantage and that copies bear this notice and the full citation on the first page. Copyrights for components of this work owned by others than the author(s) must be honored. Abstracting with credit is permitted. To copy otherwise, or republish, to post on servers or to redistribute to lists, requires prior specific permission and/or a fee. Request permissions from permissions@acm.org.

© 2025 Copyright held by the owner/author(s). Publication rights licensed to ACM.

Manuscript submitted to ACM

However, in more realistic scenarios, the differences between anomalous and normal samples are often subtle. Anomalies may manifest as sparse local information, while the rest of the information remains indistinguishable from that of normal samples. As a result, anomalous samples are highly similar to normal ones at a macro level, making them difficult to identify. For example, as illustrated in fig. 1, in a real-world customer service quality inspection task, the goal is to detect instances of impoliteness within extended conversations between customer services and customers. Since the customer service is well-trained, mistakes—if any—typically occur in only a subtle utterance.

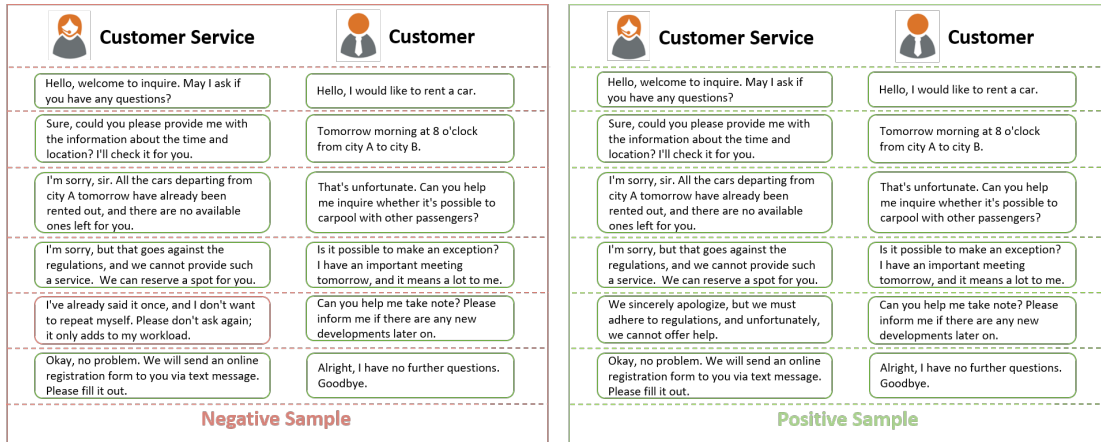


Fig. 1. This example illustrates the difficulty in distinguishing between normal and anomalous macro samples due to the low proportion of anomalous information within anomalous samples.

Given the difficulty of distinguishing samples at the macro level, a promising approach is to seek solutions at the micro level—by decomposing each macro-level sample into multiple finer-grained components and performing discrimination at this finer resolution. However, such approaches face two major challenges. First, there are no precise labels available at the micro level, so learning must rely solely on macro-level supervision. Second, anomalous samples are already scarce at the macro level [5, 23, 25], and within each anomalous sample, truly anomalous information often constitutes only a small fraction. This results in a severe imbalance along two dimensions at both the macro and the micro level, posing significant challenges for effective learning.

Multiple Instance Learning (MIL) is a paradigm of weakly supervised learning designed for scenarios with imprecise labels [9, 34, 37]. It structures data into two hierarchical levels: the macro level (referred to as bags) and the micro level (referred to as instances), and utilizes only macro-level labels for training. To address the lack of micro-level supervision, existing MIL methods often heuristically assign bag labels to all instances within the bag [2, 15, 23]. However, this strategy lacks theoretical grounding and can introduce substantial bias. In terms of data imbalance, the micro-level imbalance—known in MIL literature as the low witness rate problem—has been recognized but remains unresolved [4, 36]. Meanwhile, macro-level imbalance has been largely overlooked and presents an even greater challenge.

In this paper, instead of directly assigning bag labels to instances, we treat all instances from normal bags as positive instances and all instances from anomalous bags as unlabeled instances. This reformulates the MIL problem as a fine-grained Positive-Unlabeled (PU) learning task. PU learning is a learning paradigm that trains models using only positive and unlabeled data [3]. Its core assumption is that both labeled and unlabeled positive instances are drawn from the same underlying distribution, which enables estimation of the distribution of negative instances within the unlabeled

set and thus facilitates the separation of positive and negative instances—thereby alleviating the label bias challenge in MIL [7, 18]. Building upon this reformulation, we further derive a PU learning loss function based on rigorous theoretical analysis, which simultaneously addresses imbalance at both the macro and micro levels—thereby alleviating the dual imbalance challenge in MIL.

To develop a PU learning algorithm better suited for addressing MIL problems, we further incorporate macro-level information into the micro-level learning process. Specifically, we restrict the assignment of pseudo-labels to only high-confidence unlabeled instances, and dynamically adjust the confidence threshold to maintain balanced prediction. This design enables the model to improve macro-level performance directly through micro-level learning. The resulting algorithm, termed Balanced Fine-Grained Positive-Unlabeled (BFGPU), is a PU learning method tailored for solving MIL problems.

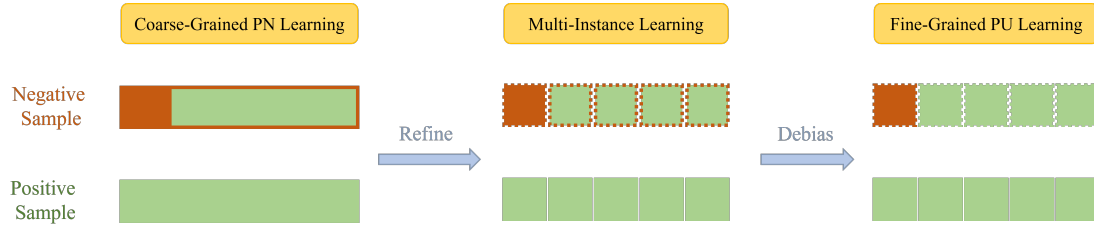


Fig. 2. This figure illustrates the different solution paradigms for the detection problem in this paper: coarse-grained positive-negative learning, MIL, and fine-grained positive-unlabeled learning.

We conducted extensive experiments to evaluate the performance of BFGPU across various datasets, including 2 datasets with a maximum imbalance ratio of 5 and 2 datasets with a maximum imbalance ratio of 10. Additionally, we tested the algorithm on a real-world customer service quality inspection dataset. These experiments demonstrated the effectiveness of BFGPU in both diverse datasets and practical applications. Furthermore, we explored scenarios with both macro and micro imbalances, and even in extreme cases where anomalous information is vastly outnumbered, our algorithm consistently performed well.

Our Contributions. 1. We propose a novel perspective that reformulates the MIL problem as a balanced PU learning task, which addresses the issues of bias and imbalance in MIL. 2. We incorporate macro information into the learning process, leading to BFGPU, an algorithm that enables balanced and unbiased macro performance by training at the micro level. 3. We provide a theoretical analysis demonstrating the advantages of BFGPU over macro-level learning and conventional MIL approaches. 4. Extensive experiments validate the superior performance of BFGPU.

2 Related Works

2.1 Positive Unlabeled Learning

PU learning can utilize positive data and unlabeled data to train a classifier that distinguishes between positive and negative data [3]. It is reasonable to use the loss of unlabeled data, proportionally subtracted from the loss of positive data, to estimate the loss of negative data. Most PU learning algorithms aim for the model to be unbiased in terms of accuracy, and there are many effective algorithms currently available [6, 7, 12–14, 16, 18, 29, 30, 33]. Some PU learning algorithms address the issue of imbalance in the positive-negative ratio within unlabeled data and strive for unbiased average accuracy (AvgAcc) [32]. Additionally, theoretical research on PU learning has demonstrated its superiority over PN learning under certain conditions [21].

2.2 Multi-Instance Learning

Multi-instance learning (MIL) is a form of weakly supervised learning [37] characterized by inexact supervision, where labels are not precise [4]. In MIL, a single label is assigned to a bag of instances, addressing the problem we are discussing. In the past, MIL approaches typically involved pooling or attention mechanisms to fuse embeddings or setting up scoring functions [1, 8, 15, 23, 25, 26]. In our case, we aim to transform this problem into a direct micro PU learning problem to achieve more accurate solutions and eliminate redundant information.

2.3 Anomaly Detection

Anomaly Detection (AD) is referred to as the process of detecting data instances that significantly deviate from the majority of data instances [5, 22]. Historically, AD methods have been categorized into supervised AD [11], weakly supervised AD [23, 25, 28], and unsupervised AD [27, 35]. However, there hasn't been a specific AD algorithm tailored for the PU form, where only normal samples are labeled and there are no labeled anomalies. Therefore, existing methods cannot be used to address the proposed problem, as macro AD and macro PN classification are similarly ineffective due to high similarity.

3 Derivation of Unbiased and Balanced PU Learning

In classical supervised learning problems, we often deal with positive-negative (PN) learning. Assume there is an underlying distribution $p(x, y)$, where $x \in \mathbb{R}^d$ is the input, and $y \in \{-1, +1\}$ is the output. Data of size n_+ are sampled from $p(x|y = +1)$, and data of size n_- are sampled from $p(x|y = -1)$. We let $g : \mathbb{R}^d \rightarrow \mathbb{R}^2$ be a decision function from a function space \mathcal{G} , where g_{-1} and g_{+1} are the probabilities of the sample being negative and positive, respectively. We also let $\mathcal{L} : \mathbb{R}^d \times \{-1, +1\} \rightarrow \mathbb{R}$ be a loss function. The goal of PN learning is to use P data and N data to learn a classifier, denoted as $f : \mathbb{R}^d \rightarrow \{-1, +1\}$ which is based on the decision function g .

However, in some scenarios, we may only have labels for one class, either only positive class labels known as PU learning or only negative class labels known as Negative-Unlabeled (NU) learning which is equivalent. In PU learning, data of size n_+ is sampled from $p(x|y = +1)$, and data of size n_u is sampled from $p(x)$. The goal is also to learn a classifier $f : \mathbb{R}^d \rightarrow \{-1, +1\}$ which is the same as PN learning. We let $\pi = p(y = +1)$ represent the class prior of the positive data. The learning objective $R_{pn}(g) = E_{p(x,y)}[\mathcal{L}[(g(x), y)]]$ of PN learning can be decomposed as

$$R_{pn}(g) = (1 - \pi)E_{p(x|y=-1)}[\mathcal{L}[g(x), -1]] + \pi E_{p(x|y=+1)}[\mathcal{L}[g(x), +1]]. \quad (1)$$

Du Plessis et al. [7] derived an unbiased PU (uPU) learning objective. Kiryo et al. [18] propose non-negative PU (nnPU), avoiding the situation in uPU where the non-negative part of the loss is negative. In them, due to the absence of labeled negative samples for PU learning, the term $E_{p(x|y=-1)}[\mathcal{L}[g(x), -1]]$ cannot be directly estimated. However, since

$$E_{p(x)}[\mathcal{L}[g(x), -1]] = (1 - \pi)E_{p(x|y=-1)}[\mathcal{L}[g(x), -1]] + \pi E_{p(x|y=+1)}[\mathcal{L}[g(x), -1]], \quad (2)$$

where π is the proportion of positive samples, $E_{p(x|y=-1)}[\mathcal{L}[g(x), -1]]$ can be indirectly estimated by leveraging the unlabeled data to estimate $E_{p(x)}[\mathcal{L}[g(x), -1]]$ and using positive data to estimate $E_{p(x|y=+1)}[\mathcal{L}[g(x), -1]]$. So the empirical unbiased PU learning loss can be estimated using the current model's prediction \hat{g} as

$$\hat{R}_{upu}(\hat{g}) = \frac{\pi}{n_p} \sum_{x_i \in P} \mathcal{L}[\hat{g}(x_i), +1] + \frac{1}{n_u} \sum_{x_i \in U} \mathcal{L}[\hat{g}(x_i), -1] - \frac{\pi}{n_p} \sum_{x_i \in P} \mathcal{L}[\hat{g}(x_i), -1]. \quad (3)$$

Table 1. The table presents the AvgAcc of different algorithms under varying values of $\sigma_{\text{micro}} \in \{2, 3, 4, 5\}$, along with the estimated AUC concerning changes in AvgAcc on the Imdb Dataset.

Method	AvgAcc				AUC_{AvgAcc}	
	2	3	4	5		
Macro	PN	76.75 ± 1.45	70.62 ± 0.83	62.61 ± 4.70	58.33 ± 4.81	67.08
	DeepSAD	52.17 ± 0.56	52.57 ± 1.20	55.01 ± 1.05	50.76 ± 0.77	52.63
	ATT	82.58 ± 7.37	85.98 ± 1.32	80.66 ± 3.81	78.62 ± 1.54	81.96
MIL	FGSA	82.67 ± 1.60	63.60 ± 13.43	60.49 ± 14.59	58.64 ± 14.97	66.35
	PRENET	84.53 ± 1.50	80.54 ± 1.50	71.78 ± 4.97	73.56 ± 2.49	77.60
	DeepSAD	62.86 ± 4.33	60.00 ± 1.43	57.80 ± 1.46	56.84 ± 0.12	59.38
Micro	DeepSVDD	52.70 ± 0.61	51.73 ± 1.13	51.96 ± 0.09	51.76 ± 2.58	52.04
	uPU	82.93 ± 1.14	76.30 ± 1.51	78.57 ± 5.37	72.29 ± 3.30	77.52
	nnPU	84.53 ± 1.49	58.39 ± 5.95	50.00 ± 0.00	50.00 ± 0.00	60.73
	balancedPU	85.78 ± 1.39	77.39 ± 3.90	84.85 ± 1.14	78.77 ± 4.17	81.70
	robustPU	87.82 ± 0.37	86.63 ± 1.11	85.49 ± 0.45	72.58 ± 19.57	83.13
	BFGPU	88.13 ± 1.07	87.93 ± 0.58	86.02 ± 0.69	83.64 ± 0.78	86.43

Su et al. [32] argued that previous approaches struggle with balanced metrics. The objective of unbiased PU learning is to train a classifier that is unbiased when the class distribution of the test data matches that of the unlabeled data, rather than creating a balanced classifier. This can lead to poor performance for one of the classes, especially when π is close to 0 or 1. In such cases, even if the model classifies all samples into a single class, achieving high accuracy, it does not meet the goals for real-world applications. Our objective is to learn a balanced classifier, despite the imbalance between positive and negative data in the unlabeled set. Building on the balanced PN learning objective, we aim to address this challenge:

$$\hat{R}_{bpn}(g) = \frac{1}{2} E_{p(x|y=+1)} [\mathcal{L}[g(x), +1]] + \frac{1}{2} E_{p(x|y=-1)} [\mathcal{L}[g(x), -1]], \quad (4)$$

Through empirical estimation, we can get the balanced PU learning objective:

$$\begin{aligned} \hat{R}_{bpu}(\hat{g}) &= \frac{1}{2n_p} \sum_{x_i \in P} \mathcal{L}[\hat{g}(x_i), +1] + \frac{1}{2n_u(1-\pi)} \sum_{x_i \in U} \mathcal{L}[\hat{g}(x_i), -1] \\ &\quad - \frac{\pi}{2n_p(1-\pi)} \sum_{x_i \in P} \mathcal{L}[\hat{g}(x_i), -1]. \end{aligned} \quad (5)$$

Theoretically, the loss function most related to accuracy is the 0-1 loss. A surrogate loss function that is unbiased with respect to the 0-1 loss should satisfy the condition $\mathcal{L}[t, +1] + \mathcal{L}[t, -1] = 1$. We directly set $\mathcal{L}[\hat{g}(x_i), -1] = 1 - \mathcal{L}[\hat{g}(x_i), +1]$ in $\hat{R}_{bpu}(g)$, yielding a simplified expression:

$$\hat{R}_{bpu}(g) = \frac{1}{2n_p(1-\pi)} \sum_{x_i \in P} \mathcal{L}[\hat{g}(x_i), +1] + \frac{1}{2n_u(1-\pi)} \sum_{x_i \in U} \mathcal{L}[\hat{g}(x_i), -1] - \frac{\pi}{2(1-\pi)}. \quad (6)$$

This simple formula illustrates a straightforward yet counterintuitive principle. When the loss function satisfies $\mathcal{L}[t, +1] + \mathcal{L}[t, -1]$ as a constant, directly treating unlabeled samples as negative and training the model using the expected loss for each class supervisely results in a balanced learner. In other words, the model becomes unbiased with respect to the average accuracy metric. Building on this, we further derive the micro-level learning objective for PU learning.

Table 2. The table presents the AvgAcc of different algorithms under varying values of $\sigma_{\text{micro}} \in \{2, 4, 6, 8, 10\}$, along with the estimated AUC concerning changes in AvgAcc on the SST-2 Dataset.

Methods		AvgAcc					AUC_{AvgAcc}
		2	4	6	8	10	
Macro	PN	83.15 ± 0.98	78.38 ± 1.02	76.57 ± 3.42	71.38 ± 9.29	73.26 ± 2.51	76.55
	DeepSAD	76.52 ± 0.23	59.41 ± 6.75	52.17 ± 1.02	49.69 ± 3.47	50.39 ± 2.19	57.64
MIL	ATT	80.76 ± 1.57	70.96 ± 3.72	57.49 ± 12.35	50.00 ± 0.00	51.16 ± 2.01	60.07
	FGSA	68.05 ± 16.87	50.00 ± 0.00	50.00 ± 0.00	50.00 ± 0.00	50.00 ± 0.00	53.61
Micro	PReNET	78.82 ± 6.43	67.33 ± 3.25	66.49 ± 3.32	56.92 ± 6.07	60.47 ± 3.49	66.00
	DeepSAD	61.33 ± 5.75	51.16 ± 1.53	48.79 ± 1.49	49.06 ± 0.77	49.22 ± 0.55	51.91
Micro	DeepSVDD	48.62 ± 1.93	50.00 ± 2.97	49.52 ± 0.42	49.06 ± 0.94	50.00 ± 1.16	49.44
	uPU	80.02 ± 1.92	71.29 ± 3.86	69.81 ± 2.80	67.92 ± 4.00	53.88 ± 2.74	68.58
	nnPU	81.49 ± 0.00	50.17 ± 0.00	50.00 ± 0.00	50.00 ± 0.00	50.00 ± 0.00	56.33
	balancedPU	77.90 ± 7.82	75.74 ± 8.49	65.70 ± 11.42	54.72 ± 3.85	57.75 ± 10.96	66.36
	robustPU	86.28 ± 1.39	75.91 ± 9.20	74.15 ± 6.16	61.64 ± 11.80	55.42 ± 9.40	70.68
	BFGPU	88.40 ± 0.68	82.51 ± 0.62	82.13 ± 0.90	79.56 ± 1.60	82.56 ± 1.64	83.03

4 Balanced Fine-Grained PU Learning

4.1 Micro-to-Macro Optimization

In the problems we encounter, the key information that determines a sample as anomalous represents only a small portion of the anomalous samples. Specifically, all local components within the normal samples do not contain anomalous information, while in the anomalous samples, apart from a small amount of local anomalous information, the rest is normal information. We are given a macro dataset $D_{\text{macro}} = \{(X_1, Y_1), \dots, (X_{|D_{\text{macro}}|}, Y_{|D_{\text{macro}}|})\}$. It can be represented separately as P_{macro} and N_{macro} . For a macro sample of length l : $X_i = [x_{i1}, x_{i2}, \dots, x_{il}]$, $x_{ij} \in \mathbb{R}^d$, $j \in [1, l]$ is the input, and $Y_i = F([y_{i1}, y_{i2}, \dots, y_{il}])$, $y_{ij} \in \{-1, +1\}$ is the output where F is the function that transforms micro labels into macro labels which constitutes a MIL problem [4]:

$$F([y_{i1}, \dots, y_{il}]) = \begin{cases} +1, & \forall j \in \{1, \dots, l\}, y_{ij} = +1 \\ -1, & \exists j \in \{1, \dots, l\}, y_{ij} = -1 \end{cases} \quad (7)$$

We denote G as the macro decision function which is transformed from the micro decision function g . Based on the relationship between the micro classifier f and the macro classifier F , that is, within a set of macro data, if all micro-components belong to the normal class, the macro label is normal; if there exists at least one anomalous component, the macro label is anomalous. This can be reformulated as another description: if the micro component most inclined towards the anomalous class is anomalous, then the macro label is anomalous; otherwise, the macro label is normal. If such a micro component can be found through g which is the idealized decision function, G can be defined:

$$G([g(x_{i1}), g(x_{i2}), \dots, g(x_{il})]) = \sum_{j=1}^l p(j = \arg \max_k g_{-1}(x_{ik})) g(x_{ij}) \quad (8)$$

Referring to eq. (8), we aim to find the idealized p which makes $p(j = \arg \max_k g_{-1}(x_{ik})) = \mathbb{I}[j = \arg \max_k g_{-1}(x_{ik})]$. However, since we cannot obtain g , during the training process of neural networks, \hat{g} from the neural network often deviates somewhat from the ideal decision function g . Consequently, we cannot directly obtain the value of the indicator function $\mathbb{I}[j = \arg \min_k g_{-1}(x_{ik})]$, but we can estimate the probability of the condition being satisfied. So, we use the

probability function \hat{p} instead of the function p .

$$\hat{p}(x_{ij}) = \frac{\exp(\hat{g}_{-1}(x_{ij}))}{\sum_{k=1}^l \exp(\hat{g}_{-1}(x_{ik}))} \quad (9)$$

Given our task, we are no longer pursuing the performance of the PU learning model at the micro level. Our ultimate goal is to ensure that the model trained at the micro level is beneficial for macro learning. We define the unbiased and balanced coarse-grained PN learning objective for the model as

$$\begin{aligned} \hat{R}_{cgpn}(\hat{g}) = & \frac{1}{2 \cdot |P_{macro}| \cdot l} \sum_{X_i \in P_{macro}} \mathcal{L}[G([\hat{g}(x_{i1}), \dots, \hat{g}(x_{il})]), +1] \\ & + \frac{1}{2 \cdot |N_{macro}| \cdot l} \sum_{X_i \in N_{macro}} \mathcal{L}[G([\hat{g}(x_{i1}), \dots, \hat{g}(x_{il})]), -1] \end{aligned} \quad (10)$$

Based on eqs. (6) and (8) to (10), through the transformation of the learning paradigm, we derive a loss function that enables unbiased and balanced optimization of macro-level performance directly at the micro level which is called balanced fine-grained PU learning loss:

$$\begin{aligned} \hat{R}_{cgpn}(\hat{g}) = \hat{R}_{bfgpu}(\hat{g}) = & \frac{1}{2|P_{micro}|} \sum_{x_{ij} \in P_{micro}} \hat{p}(x_{ij}) \mathcal{L}[\hat{g}(x_{ij}), +1] \\ & + \frac{1}{2|U_{micro}|} \sum_{x_{ij} \in U_{micro}} \hat{p}(x_{ij}) \mathcal{L}[\hat{g}(x_{ij}), -1] \end{aligned} \quad (11)$$

4.2 Pseudo Labels Based on Macro Information

After an epoch of PU learning, the model has acquired some discriminative ability for normal and anomalous samples. Further training with PN learning can be considered by obtaining pseudo-labels from unlabeled data. In the previous stage, we only utilized the micro information of the samples, neglecting the macro information. In the new stage, we can leverage this macro information. For an anomalous macro sample, since we know it contains at least one anomalous micro sample, we can directly label the most inclined-to-anomalous micro sample as an anomalous sample. Additionally, to ensure the balance of the learner, we simultaneously label the most inclined-to-normal micro sample as a normal sample. This way, we obtain an equal number of positive and negative pseudo-labeled samples for further model training. Expressed symbolically as:

$$N_{pse} = \{(x_{ij}, -1), j = \arg \max_k \hat{g}_{-1}(x_{ik}), X_i \in N_{macro}\} \quad (12)$$

$$P_{pse} = \{(x_{ij}, +1), j = \arg \min_k \hat{g}_{-1}(x_{ik}), X_i \in N_{macro}\} \quad (13)$$

Then we use N_{pse} and P_{pse} to further train the model. This ensures the improvement while maintaining the balance between positive and negative samples. The loss function is:

$$\hat{R}_{pse}(\hat{g}) = \sum_{(x_i, y_i) \in N_{pse} + P_{pse}} \mathcal{L}[\hat{g}(x_i), y_i] \quad (14)$$

4.3 Adjusted Decision Threshold (ADT)

After the training is completed, we deploy the model for testing. During the learning process, it is necessary to set an appropriate threshold. The final label is determined by comparing the decision function with the threshold. Typically, a default threshold of 0.5 is assumed, but a more precise threshold can be determined by using the normal label distribution

$\pi = 1 - \frac{1}{(\sigma_{micro}+1) \cdot (\sigma_{macro}+1)}$. Here, $\sigma_{micro} = (l - 1)$ and $\sigma_{macro} = \frac{|P_{macro}|}{|N_{macro}|}$ denote the imbalance ratios of the MIL problem at the micro and macro levels, respectively. Since we have access to the decision function values $\hat{g}(x)$, for all micro-unlabeled samples, it is sufficient to sort $\hat{g}(x)_{-1}$ in ascending order. After sorting, we can choose the position that corresponds to π as the threshold T :

$$T = \text{sort}([\hat{g}_{-1}(x_i), x_i \in U_{micro}])[\lfloor |U_{micro}| \cdot \pi \rfloor] \quad (15)$$

This approach helps determine an accurate threshold because the decision function $g(x)$ reflects the conditional probability $p(y|x)$. $p(y|x)$ remains consistent between training and testing data. Therefore, the threshold obtained on the unlabeled data is highly applicable to the test data. The overall process of the algorithm can be seen in algorithm 1.

5 Experiments

5.1 Experimental Settings

All experiments were conducted using the Roberta model as the base model [19], Adam as the optimizer [17], with a learning rate set to 10^{-5} , and CosineAnnealingLR as the learning rate scheduler. The number of epochs was set to 5, batch size to 16, and all experiments were repeated 3 times with random seeds [0, 1, 2] to obtain the mean and variance of performance. We denote σ_{micro} as the imbalance ratio at the micro level, which represents the positive-negative ratio of micro samples in negative macro samples. σ_{macro} represents the imbalance ratio at the macro level, which is the ratio of positive macro samples to negative macro samples. We set $\lambda_{bfgpu} = 1/\pi$ and $\lambda_{pse} = 1$ in all experiments. For public datasets, a macro-level normal sample is composed of $\sigma_{micro} + 1$ positive instances, while a macro-level anomalous sample is composed of σ_{micro} positive instances and 1 negative instance. In the experiments in sections 5.3, 5.4 and 5.6, σ_{macro} was set to 1, while in the experiments in section 5.5, σ_{macro} was set to 5. σ_{micro} was set to [2, 4, 6, 8, 10] for short texts and [2, 3, 4, 5] for moderate texts. In section 5.4, σ_{micro} varied inconsistently averaging around 25. For micro-level PU learning, $\pi = \frac{\sigma_{micro}}{\sigma_{micro}+1}$. The algorithms were implemented using the PyTorch framework [24]. We used average accuracy and F1 score, two commonly used evaluation metrics in imbalanced learning. Regarding the F1 score, when dealing with class imbalance problems, we typically focus on the performance of the minority (anomalous) class. We also compared the algorithm performance as σ_{micro} varies, using the area under the curve AUC_{AvgAcc} and AUC_{F1} . 4 A800 GPUs are used for all experiments.

5.2 Compared Methods

Our comparative algorithms consist of: **Macro PN**: Conventional macro binary classification. **Macro DeepSAD**: Supervised macro AD using DeepSAD [28]. **Micro DeepSAD**: Supervised micro AD, using DeepSAD [28] and treating unlabeled samples as negative class. **Micro DeepSVDD**: Unsupervised micro AD, using DeepSVDD [27] which is an One-Class Classification (OCC) method using only positive samples. **Micro Multi-Instance Learning**: Multi-instance learning algorithms used to address inexact supervision, using three multi-instance learning algorithms MIL-ATT [15], MIL-FGSA [2], and MIL-PreNET [23] which are suitable for text data. **Micro PU Learning**: Utilizing four types of loss functions uPU [7], nnPU [18], balancedPU [32], and robustPU [38] for micro-level PU learning.

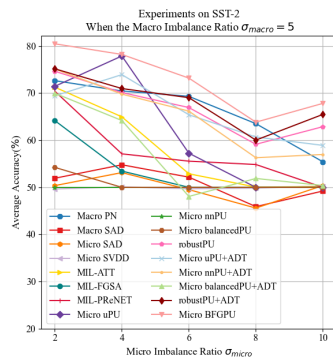


Fig. 3. The figure presents the AvgAcc of different algorithms under both micro and macro imbalance on SST-2.

Table 3. Experiments on Customer Service Quality Inspection Dataset in the Real Application.

	Method	AvgAcc	F1 Score
Macro	PN	52.38 ± 4.12	8.33 ± 14.33
	DeepSAD	47.61 ± 4.12	6.67 ± 11.55
MIL	ATT	54.76 ± 11.48	53.27 ± 8.72
	FGSA	53.57 ± 7.14	54.14 ± 9.12
	PReNET	59.52 ± 2.06	59.05 ± 0.86
Micro	DeepSAD	58.33 ± 5.46	63.12 ± 4.89
	DeepSVDD	50.00 ± 0.00	0.00 ± 0.00
	uPU	50.00 ± 0.00	0.00 ± 0.00
	nnPU	50.00 ± 0.00	0.00 ± 0.00
	balancedPU	50.00 ± 0.00	0.00 ± 0.00
	robustPU	50.00 ± 0.00	0.00 ± 0.00
	BFGPU	71.43 ± 9.45	75.31 ± 5.84

5.3 Experiments with Public Datasets

We conducted experiments with 2 datasets with small imbalanced ratios: IMDB [20], Amazon, and 2 with large ones: SST-2 [31], Sentiment140 [10]. We present the AvgAcc results on the SST-2 and IMDB datasets in tables 1 and 2. The remaining experimental results can be found in tables 4 to 7, which are in the appendix.

5.4 Experiments in the Real Application

In a real-world application, we evaluated with a customer service quality inspection dataset depicted in fig. 1. The dataset consists of instances where service personnel were flagged for substandard performance during service. The results are shown in table 3.

5.5 Experiments with Imbalance at Both Level

We considered a more extreme scenario where the normal-anomalous ratio at not only the micro but also the macro level is imbalanced. The imbalance lead to the anomalous information accounting for only $\frac{1}{(1+\sigma_{micro}) \cdot (1+\sigma_{macro})}$. However, our algorithm still achieved outstanding performance. We set σ_{macro} to 5 and conducted the experiment on the SST-2 dataset. The experimental results are shown in table 8 in the appendix. We plotted the curve of average accuracy varying as shown in section 5.2.

5.6 Ablation Study

To validate the necessity of each component of BFGPU, we conducted ablation experiments. In addition to the comprehensive algorithm, we considered 3 settings: Not using the balanced fine-grained PU learning loss function; Not using pseudo-labeling for further training; Not using adjusted thresholds. The results on the datasets IMDB and SST-2 are shown in table 9 and table 10 respectively.

5.7 Sensitivity Analysis

BFGPU mainly has two hyperparameters, λ_{bfgpu} and λ_{pse} . To validate the stability under different hyperparameter settings, we conducted a sensitivity analysis using the SST-2 dataset. The results of λ_{bfgpu} and λ_{pse} are shown in table 11 and table 12 respectively.

5.8 Analysis of Results

All results pointed to some common conclusions: balanced fine-grained PU learning outperformed coarse-grained PN learning and MIL; in most cases, BFGPU is more suitable for the MIL problem than other PU methods; in real-world and extremely imbalanced scenarios, BFGPU is irreplaceable. The ablation experiments demonstrate that the absence of each component of the algorithm framework significantly reduces the overall performance. The sensitivity analysis shows that BFGPU performs sufficiently well and is less dependent on the hyperparameters.

6 Theoretical Argumentation

We conducted analyses of the generalization error bounds for coarse-grained PN learning, MIL, and balanced fine-grained PU learning, identifying their respective applicability ranges. We also pointed out the necessity of adopting the micro PU learning paradigm, especially when the abnormal content is low. The theoretical analysis below is based on two assumptions [21]:

ASSUMPTION 1. *There is a constant $C_{\mathcal{G}} > 0$ such that: $\mathcal{R}_{n,q}(\mathcal{G}) \leq C_{\mathcal{G}}/\sqrt{n}$ where $\mathcal{R}_{n,q}(\mathcal{G})$ is the Rademacher complexity of the function space \mathcal{G} for n samples from any marginal distribution $q(x)$.*

ASSUMPTION 2. *The loss function L satisfies the symmetric condition and α_L -Lipschitz continuity:*

$$L(t, +1) + L(t, -1) = 1, |L(t_1, y) - L(t_2, y)| \leq \alpha_L |t_1 - t_2| \quad (16)$$

At the macro level, the average generalization error bound for all classes under normal circumstances is relatively easy to infer. However, due to the issue of extremely low abnormal class information in abnormal class samples, as much as $\frac{l-1}{l}$ of the information in the classification task samples can be redundant or even considered as noise. Therefore, the generalization error bound of coarse-grained PN (CGPN) learning that we derive is:

THEOREM 1. *For any $\delta > 0$, with probability at least $1 - \delta$:*

$$\begin{aligned} \hat{R}(g_{cgpn}) - R(g^*) &\leq \frac{2 \cdot (\sigma_{macro} + 1) \cdot \sqrt{\sigma_{micro+1}} \cdot \alpha_L \cdot C_{\mathcal{G}}}{\sigma_{macro} \cdot \sqrt{|P_{micro}|}} \\ &+ \frac{\sigma_{macro} + 1}{2 \cdot \sigma_{macro}} \cdot \sqrt{\frac{2 \cdot (\sigma_{micro} + 1) \cdot \ln(4/\delta)}{|P_{micro}|}} + \frac{2 \cdot (\sigma_{macro} + 1) \cdot \sqrt{\sigma_{micro+1}} \cdot \alpha_L \cdot C_{\mathcal{G}}}{\sqrt{|U_{micro}|}} \\ &+ \frac{\sigma_{macro} + 1}{2} \cdot \sqrt{\frac{2 \cdot (\sigma_{micro} + 1) \cdot \ln(4/\delta)}{|U_{micro}|}} + Disc(\mathcal{G}, p_1(x, y), p_{1/l}(x, y)) \end{aligned} \quad (17)$$

where $g^* = \arg \min_{g \in \mathcal{G}} R(g)$ be the optimal decision function for $p_1(x, y)$ in \mathcal{G} , and

$$Disc(\mathcal{G}, p_1(x, y), p_{1/l}) = \max_{g \in \mathcal{G}} |p_{x, y \sim p_1(x, y)}(g(x) \neq y) - p_{x, y \sim p_{1/l}(x, y)}(g(x) \neq y)| \quad (18)$$

represents the discrepancy in distribution between the effective information proportion of $1/l$ and the effective information proportion of 1 for the function set \mathcal{G} .

In classic MIL algorithms, all instances within an anomalous bag are treated as anomalous, which introduces significant bias. The extent of this bias is jointly determined by the imbalance levels at both the micro and macro levels, denoted as σ_{micro} and σ_{macro} , respectively. Therefore, the generalization error bound of MIL that we derive is:

THEOREM 2. *For any $\delta > 0$, with probability at least $1 - \delta$:*

$$\begin{aligned} \hat{R}(g_{mil}) - R(g^*) &\leq \frac{2 \cdot (\sigma_{macro} + 1) \cdot \alpha_L \cdot C_{\mathcal{G}}}{\sigma_{macro} \cdot \sqrt{|P_{micro}|}} + \frac{2 \cdot (\sigma_{macro} + 1) \cdot \alpha_L \cdot C_{\mathcal{G}}}{\sqrt{|U_{micro}|}} + \frac{\sigma_{macro} + 1}{2 \cdot \sigma_{macro}} \\ &\cdot \sqrt{\frac{2 \cdot \ln(4/\delta)}{|P_{micro}|}} + \frac{\sigma_{macro} + 1}{2} \cdot \sqrt{\frac{2 \cdot \ln(4/\delta)}{|U_{micro}|}} + p_{inc}(\mathcal{G}, g^*) + \frac{\sigma_{macro} + 1}{2} \cdot \frac{\sigma_{micro}}{\sigma_{micro} + 1} \end{aligned} \quad (19)$$

where $p_{inc}(\mathcal{G}, g^*) = \max_{g \in \mathcal{G}} p(\arg \max_j g_{-1}(x_j) \neq \arg \max_j g_{-1}^*(x_j))$ means the inconsistency between the true closest abnormal micro-sample in the macro sample and the predicted one.

Based on the derivation of the PU loss in eq. (11), we found that directly optimizing unlabeled samples as abnormal samples essentially balances the loss of PN learning. Therefore, the generalization error bound of BFGPU that we derive is:

THEOREM 3. *For any $\delta > 0$, with probability at least $1 - \delta$:*

$$\hat{R}(g_{bfgpu}) - R(g^*) \leq \frac{4 \cdot \alpha_L \cdot C_{\mathcal{G}}}{\sqrt{|P_{micro}|}} + \sqrt{\frac{2 \cdot \ln(4/\delta)}{|P_{micro}|}} + \frac{4 \cdot \alpha_L \cdot C_{\mathcal{G}}}{\sqrt{|U_{micro}|}} + \sqrt{\frac{2 \cdot \ln(4/\delta)}{|U_{micro}|}} + p_{inc}(\mathcal{G}, g^*). \quad (20)$$

The above theoretical results indicate that when the proportion of negative samples at the micro level is too low in the macro-level samples, the micro PU learning paradigm not only reduces the variance caused by model space complexity and confidence δ due to a large number of samples but also does not need to face the distribution discrepancy caused by a large amount of redundant or noisy information. BFGPU eliminates the bias in MIL, and unlike CGPN and MIL—which are heavily affected by σ_{micro} and σ_{macro} —its error bound is not influenced by the class imbalance problem.

7 Conclusion

We addressed the challenge of anomalous detection in real-world scenarios where anomalous information is extremely sparse: macroscopically, there is high similarity between normal and anomalous samples, and microscopically, labels are lacking and imbalanced. We transformed the problem into an imbalanced PU learning task at the micro level, demonstrating its feasibility through theoretical analysis. We proposed a solution that directly optimizes macro-level performance at the micro level using PU learning objectives and combined pseudo-labeling with threshold adjustment techniques to create a new framework. Experiments validated that this framework effectively tackles the issue of sparse negative information while maintaining strong performance even in extreme cases of imbalance at both macro and micro levels.

References

- [1] Davide Abati, Angelo Porrello, Simone Calderara, and Rita Cucchiara. 2019. Latent space autoregression for novelty detection. In *Proceedings of the IEEE/CVF Conference on Computer Vision and Pattern Recognition*. 481–490.
- [2] Stefanos Angelidis and Mirella Lapata. 2018. Multiple instance learning networks for fine-grained sentiment analysis. *Transactions of the Association for Computational Linguistics* 6 (2018), 17–31.
- [3] Jessa Bekker and Jesse Davis. 2020. Learning from positive and unlabeled data: A survey. *Machine Learning* 109 (2020), 719–760.
- [4] Marc-André Carboneau, Veronika Cheplygina, Eric Granger, and Ghyslain Gagnon. 2018. Multiple instance learning: A survey of problem characteristics and applications. *Pattern Recognition* 77 (2018), 329–353.
- [5] Varun Chandola, Arindam Banerjee, and Vipin Kumar. 2009. Anomaly detection: A survey. *Comput. Surveys* 41, 3 (2009), 1–58.
- [6] Xuxi Chen, Wuyang Chen, Tianlong Chen, Ye Yuan, Chen Gong, Kewei Chen, and Zhangyang Wang. 2020. Self-pu: Self boosted and calibrated positive-unlabeled training. In *Proceedings of the 37th International Conference on Machine Learning*. 1510–1519.
- [7] Marthinus Du Plessis, Gang Niu, and Masashi Sugiyama. 2015. Convex formulation for learning from positive and unlabeled data. In *Proceedings of the 32nd International Conference on Machine Learning*. 1386–1394.
- [8] Ji Feng and Zhi-Hua Zhou. 2017. Deep MIML network. In *Proceedings of the 31st AAAI Conference on Artificial Intelligence*. 1884–1890.
- [9] Wei Gao, Fang Wan, Jun Yue, Songcen Xu, and Qixiang Ye. 2022. Discrepant multiple instance learning for weakly supervised object detection. *Pattern Recognition* 122 (2022), 108233.
- [10] Alec Go, Richa Bhayani, and Lei Huang. 2009. Twitter sentiment classification using distant supervision. In *Proceedings of the 9th International Conference on Communication Systems and Networks*, Vol. 1. 2009.
- [11] Nico Görnitz, Marius Kloft, Konrad Rieck, and Ulf Brefeld. 2013. Toward supervised anomaly detection. *Journal of Artificial Intelligence Research* 46 (2013), 235–262.
- [12] Ming Hou, Brahim Chaib-Draa, Chao Li, and Qibin Zhao. 2018. Generative adversarial positive-unlabeled learning. In *Proceedings of the 27th International Joint Conference on Artificial Intelligence*. 2255–2261.
- [13] Cho-Jui Hsieh, Nagarajan Natarajan, and Inderjit Dhillon. 2015. PU learning for matrix completion. In *Proceedings of the 32nd International Conference on Machine Learning*. 2445–2453.
- [14] Yu-Guan Hsieh, Gang Niu, and Masashi Sugiyama. 2019. Classification from positive, unlabeled and biased negative data. In *Proceedings of the 36th International Conference on Machine Learning*. 2820–2829.
- [15] Maximilian Ilse, Jakub Tomczak, and Max Welling. 2018. Attention-based deep multiple instance learning. In *Proceedings of the 35th International conference on Machine Learning*. 2127–2136.
- [16] Masahiro Kato, Takeshi Teshima, and Junya Honda. 2018. Learning from positive and unlabeled data with a selection bias. In *Proceedings of the 7th International Conference on Learning Representations*.
- [17] Diederik P. Kingma and Jimmy Ba. 2015. Adam: A Method for Stochastic Optimization. In *Proceedings of the 3rd International Conference on Learning Representations*.
- [18] Ryuichi Kiryo, Gang Niu, Marthinus C Du Plessis, and Masashi Sugiyama. 2017. Positive-unlabeled learning with non-negative risk estimator. In *Advances in Neural Information Processing Systems*. 1675–1685.
- [19] Yinhan Liu, Myle Ott, Naman Goyal, Jingfei Du, Mandar Joshi, Danqi Chen, Omer Levy, Mike Lewis, Luke Zettlemoyer, and Veselin Stoyanov. 2019. Roberta: A robustly optimized bert pretraining approach. *arXiv preprint arXiv:1907.11692* (2019).
- [20] Andrew Maas, Raymond E Daly, Peter T Pham, Dan Huang, Andrew Y Ng, and Christopher Potts. 2011. Learning word vectors for sentiment analysis. In *Proceedings of the 49th Annual Meeting of the Association for Computational Linguistics: Human Language Technologies*. 142–150.
- [21] Gang Niu, Marthinus Christoffel Du Plessis, Tomoya Sakai, Yao Ma, and Masashi Sugiyama. 2016. Theoretical comparisons of positive-unlabeled learning against positive-negative learning. In *Advances in Neural Information Processing Systems*. 1199–1207.
- [22] Guansong Pang, Chunhua Shen, Longbing Cao, and Anton Van Den Hengel. 2021. Deep learning for anomaly detection: A review. *Comput. Surveys* 54, 2 (2021), 1–38.
- [23] Guansong Pang, Chunhua Shen, Huidong Jin, and Anton van den Hengel. 2023. Deep weakly-supervised anomaly detection. In *Proceedings of the 29th ACM SIGKDD Conference on Knowledge Discovery and Data Mining*. 1795–1807.
- [24] Adam Paszke, Sam Gross, Francisco Massa, Adam Lerer, James Bradbury, Gregory Chanan, Trevor Killeen, Zeming Lin, Natalia Gimelshein, Luca Antiga, et al. 2019. Pytorch: An imperative style, high-performance deep learning library. In *Advances in Neural Information Processing Systems*. 8024–8035.
- [25] Lorenzo Perini, Vincent Vercruyssen, and Jesse Davis. 2023. Learning from Positive and Unlabeled Multi-Instance Bags in Anomaly Detection. In *Proceedings of the 29th ACM SIGKDD Conference on Knowledge Discovery and Data Mining*. 1897–1906.
- [26] Pedro O Pinheiro and Ronan Collobert. 2015. From image-level to pixel-level labeling with convolutional networks. In *Proceedings of the IEEE Conference on Computer Vision and Pattern Recognition*. 1713–1721.
- [27] Lukas Ruff, Robert Vandermeulen, Nico Goernitz, Lucas Deecke, Shoaib Ahmed Siddiqui, Alexander Binder, Emmanuel Müller, and Marius Kloft. 2018. Deep one-class classification. In *Proceedings of the 35th International Conference on Machine Learning*. 4393–4402.
- [28] Lukas Ruff, Robert A Vandermeulen, Nico Görnitz, Alexander Binder, Emmanuel Müller, Klaus-Robert Müller, and Marius Kloft. 2019. Deep Semi-Supervised Anomaly Detection. In *Proceedings of the 8th International Conference on Learning Representations*.

- [29] Emanuele Sansone, Francesco GB De Natale, and Zhi-Hua Zhou. 2018. Efficient training for positive unlabeled learning. *IEEE Transactions on Pattern Analysis and Machine Intelligence* 41, 11 (2018), 2584–2598.
- [30] Hong Shi, Shaojun Pan, Jian Yang, and Chen Gong. 2018. Positive and Unlabeled Learning via Loss Decomposition and Centroid Estimation.. In *Proceedings of the 27th International Joint Conference on Artificial Intelligence*. 2689–2695.
- [31] Richard Socher, Alex Perelygin, Jean Wu, Jason Chuang, Christopher D Manning, Andrew Y Ng, and Christopher Potts. 2013. Recursive deep models for semantic compositionality over a sentiment treebank. In *Proceedings of the Conference on Empirical Methods in Natural Language Processing*. 1631–1642.
- [32] Guangxin Su, Weitong Chen, and Miao Xu. 2021. Positive-unlabeled learning from imbalanced data.. In *Proceedings of the 32nd International Joint Conference on Artificial Intelligence*. 2995–3001.
- [33] Xutao Wang, Hanting Chen, Tianyu Guo, and Yunhe Wang. 2024. Pue: Biased positive-unlabeled learning enhancement by causal inference. In *Advances in Neural Information Processing Systems*. 19783–19798.
- [34] Muhammad Waqas, Syed Umaid Ahmed, Muhammad Atif Tahir, Jia Wu, and Rizwan Qureshi. 2024. Exploring multiple instance learning (MIL): A brief survey. *Expert Systems with Applications* (2024), 123893.
- [35] Hangting Ye, Zhining Liu, Xinyi Shen, Wei Cao, Shun Zheng, Xiaofan Gui, Huishuai Zhang, Yi Chang, and Jiang Bian. 2023. UADB: Unsupervised Anomaly Detection Booster. In *Proceedings of the 12th International Conference on Learning Representations*. 18019–18042.
- [36] Hongrun Zhang, Yanda Meng, Yitian Zhao, Yihong Qiao, Xiaoyun Yang, Sarah E Coupland, and Yalin Zheng. 2022. Dtdf-mil: Double-tier feature distillation multiple instance learning for histopathology whole slide image classification. In *Proceedings of the IEEE/CVF conference on computer vision and pattern recognition*. 18802–18812.
- [37] Zhi-Hua Zhou. 2018. A brief introduction to weakly supervised learning. *National Science Review* 5, 1 (2018), 44–53.
- [38] Zhangchi Zhu, Lu Wang, Pu Zhao, Chao Du, Wei Zhang, Hang Dong, Bo Qiao, Qingwei Lin, Saravan Rajmohan, and Dongmei Zhang. 2023. Robust Positive-Unlabeled Learning via Noise Negative Sample Self-correction. In *Proceedings of the 29th ACM SIGKDD Conference on Knowledge Discovery and Data Mining*. 3663–3673.

A Algorithm Framework

The specific algorithmic framework is shown in algorithm 1.

Algorithm 1 Balanced Fine-Grained PU Learning

Training Phase

Input: macro positive dataset P_{macro} , macro negative dataset N_{macro} , the coefficient of \hat{R}_{bfgpu} λ_{bfgpu} , the coefficient of \hat{R}_{pse} λ_{pse} , learning rate η , the number of epochs E , class distribution prior π .

Output: micro classifier g , threshold T .

Split the macro-level data: $P_{micro} \leftarrow Split(P_{macro})$

Split the macro-level data: $U_{micro} \leftarrow Split(N_{macro})$

Initialize g with parameters θ

for $e = 1$ **to** E **do**

for P_{batch}, U_{batch} **in** P_{micro}, U_{micro} **do**

 Get the probabilities \hat{p} by eq. (9)

 Get the loss \hat{R}_{bfgpu} by eq. (11)

$\theta = \theta - \eta \nabla_{\theta} (\lambda_{bfgpu} \cdot \hat{R}_{bfgpu})$

end for

 Get P_{pse}, N_{pse} by eqs. (12) and (13)

for P_{batch}, N_{batch} **in** P_{pse}, N_{pse} **do**

 Get the loss \hat{R}_{pse} by eq. (14)

$\theta = \theta - \eta \nabla_{\theta} (\lambda_{pse} \cdot \hat{R}_{pse})$

end for

end for

Get the threshold T by eq. (15)

Testing Phase

Input: macro test data X_T , micro classifier g , and threshold T .

Output: macro prediction Y_T .

for X_i **in** X_T **do**

 Initial $Y_{Ti} \leftarrow +1$

for x_{ij} **in** X_i **do**

if $g_{-1}(x_{ij}) > T$ **then**

 Update $Y_{Ti} \leftarrow -1$

end if

end for

end for

B Proof of the Theories

B.1 Proof of Theorem 4.1

Consider directly learning from macro-level data at the macro level, where the proportion of effective information is $1/l$ in the macro, and then testing on data with the same proportion. It can be shown that there exists $\delta > 0$, with at least a

probability of $1 - \delta$:

$$\begin{aligned}
 & \hat{R}(g_{cgpn}) - R(g_{1/l}^*) \\
 & \leq \frac{1}{2} \cdot \left(\frac{4 \cdot \alpha_L \cdot C_{\mathcal{G}}}{\sqrt{|P_{micro}|/(\sigma_{micro} + 1)}} + \sqrt{\frac{2 \cdot \ln(4/\delta)}{|P_{micro}|/(\sigma_{micro} + 1)}} \right) / \frac{\sigma_{macro}}{\sigma_{macro} + 1} \\
 & \quad + \frac{1}{2} \cdot \left(\frac{4 \cdot \alpha_L \cdot C_{\mathcal{G}}}{\sqrt{|U_{micro}|/(\sigma_{micro} + 1)}} + \sqrt{\frac{2 \cdot \ln(4/\delta)}{|U_{micro}|/(\sigma_{micro} + 1)}} \right) / \frac{1}{\sigma_{macro} + 1}
 \end{aligned} \tag{21}$$

Then, considering the data distribution caused by redundant information differs from the data distribution when there is no redundant information, it is not difficult to conclude that:

$$R(g_{1/l}^*) - R(g^*) \leq Disc(\mathcal{G}, p_1(x, y), p_{1/l}(x, y)) \tag{22}$$

By combining the two equations, we can measure the gap between the macro PN error and the error of the optimal classifier at the macro level when there is no redundant information. Ultimately proved for any $\delta > 0$, with probability at least $1 - \delta$:

$$\begin{aligned}
 & \hat{R}(g_{cgpn}) - R(g^*) \\
 & = (\hat{R}(g_{cgpn}) - R(g_{1/l}^*)) + (R(g_{1/l}^*) - R(g^*)) \\
 & \leq \frac{2 \cdot (\sigma_{macro} + 1) \cdot \sqrt{\sigma_{micro} + 1} \cdot \alpha_L \cdot C_{\mathcal{G}}}{\sigma_{macro} \cdot \sqrt{|P_{micro}|}} \\
 & \quad + \frac{\sigma_{macro} + 1}{2 \cdot \sigma_{macro}} \cdot \sqrt{\frac{2 \cdot (\sigma_{micro} + 1) \cdot \ln(4/\delta)}{|P_{micro}|}} + \frac{2 \cdot (\sigma_{macro} + 1) \cdot \sqrt{\sigma_{micro} + 1} \cdot \alpha_L \cdot C_{\mathcal{G}}}{\sqrt{|U_{micro}|}} \\
 & \quad + \frac{\sigma_{macro} + 1}{2} \cdot \sqrt{\frac{2 \cdot (\sigma_{micro} + 1) \cdot \ln(4/\delta)}{|U_{micro}|}} + Disc(\mathcal{G}, p_1(x, y), p_{1/l}(x, y))
 \end{aligned} \tag{23}$$

B.2 Proof of Theorem 4.2

Consider assigning the macro-level labels to all micro-level samples. For normal samples, all training labels are correct; whereas for anomalous samples, the upper bound of labeling error is $\frac{\sigma_{micro}}{\sigma_{micro} + 1}$. When the class imbalance ratio at the macro level is σ_{macro} , it is straightforward to derive the balanced error upper bound for training with the MIL method. It can be shown that there exists $\delta > 0$, with at least a probability of $1 - \delta$:

$$\begin{aligned}
 & \hat{R}(g_{mil}) - R(g_{micro}^*) \\
 & \leq \frac{1}{2} \cdot \left(\frac{4 \cdot \alpha_L \cdot C_{\mathcal{G}}}{\sqrt{|P_{micro}|}} + \sqrt{\frac{2 \cdot \ln(4/\delta)}{|P_{micro}|}} \right) / \frac{\sigma_{macro}}{\sigma_{macro} + 1} \\
 & \quad + \frac{1}{2} \cdot \left(\frac{4 \cdot L_l \cdot C_{\mathcal{G}}}{\sqrt{|U_{micro}|}} + \sqrt{\frac{2 \cdot \ln(4/\delta)}{|U_{micro}|}} + \frac{\sigma_{micro}}{\sigma_{micro} + 1} \right) / \frac{1}{\sigma_{macro} + 1}
 \end{aligned} \tag{24}$$

Considering the inconsistency between micro-level optimization goals and macro-level optimization goals, it is not difficult to conclude that:

$$R(g_{micro}^*) - R(g^*) \leq p_{inc}(\mathcal{G}, g^*) \quad (25)$$

By combining the two equations, we can measure the gap between the MIL error and the error of the optimal classifier at the macro level. Ultimately proved for any $\delta > 0$, with probability at least $1 - \delta$: For any $\delta > 0$, with probability at least $1 - \delta$:

$$\begin{aligned} & \hat{R}(g_{mil}) - R(g^*) \\ &= (\hat{R}(g_{mil}) - R(g_{micro}^*)) + (R(g_{micro}^*) - R(g^*)) \\ &\leq \frac{2 \cdot (\sigma_{macro} + 1) \cdot \alpha_L \cdot C_{\mathcal{G}}}{\sigma_{macro} \cdot \sqrt{|P_{micro}|}} + \frac{2 \cdot (\sigma_{macro} + 1) \cdot \alpha_L \cdot C_{\mathcal{G}}}{\sqrt{|U_{micro}|}} + \frac{\sigma_{macro} + 1}{2 \cdot \sigma_{macro}} \cdot \sqrt{\frac{2 \cdot \ln(4/\delta)}{|P_{micro}|}} \\ &\quad + \frac{\sigma_{macro} + 1}{2} \cdot \sqrt{\frac{2 \cdot \ln(4/\delta)}{|U_{micro}|}} + p_{inc}(\mathcal{G}, g^*) + \frac{\sigma_{macro} + 1}{2} \cdot \frac{\sigma_{micro}}{\sigma_{micro} + 1} \end{aligned} \quad (26)$$

B.3 Proof of Theorem 4.3

By directly optimizing the balanced PU loss at the micro level, we can achieve unbiased optimization of macro-level performance. Taking into account the error introduced by converting the macro-level problem to the micro level, we ultimately obtain an error upper bound for BFGPU that is independent of both imbalance ratios σ_{macro} and σ_{micro} . It can be shown that there exists $\delta > 0$, with at least a probability of $1 - \delta$:

$$\begin{aligned} & \hat{R}(g_{bfgpu}) - R(g_{micro}^*) \\ &\leq \frac{4 \cdot L_l \cdot C_{\mathcal{G}}}{\sqrt{|P_{micro}|}} + \frac{4 \cdot L_l \cdot C_{\mathcal{G}}}{\sqrt{|U_{micro}|}} \\ &\quad + \sqrt{\frac{2 \cdot \ln(4/\delta)}{|P_{micro}|}} + \sqrt{\frac{2 \cdot \ln(4/\delta)}{|U_{micro}|}} \end{aligned} \quad (27)$$

Considering the inconsistency between micro-level optimization goals and macro-level optimization goals, it is not difficult to conclude that:

$$R(g_{micro}^*) - R(g^*) \leq p_{inc}(\mathcal{G}, g^*) \quad (28)$$

By combining the two equations, we can measure the gap between the micro PU error and the error of the optimal classifier in the marco level when there is no redundant information. Ultimately proved for any $\delta > 0$, with probability at least $1 - \delta$: For any $\delta > 0$, with probability at least $1 - \delta$:

$$\begin{aligned}
& \hat{R}(g_{bfgpu}) - R(g^*) \\
&= (\hat{R}(g_{bfgpu}) - R(g_{micro}^*)) + (R(g_{micro}^*) - R(g^*)) \\
&\leq \frac{4 \cdot L_I \cdot C_{\mathcal{G}}}{\sqrt{|P_{micro}|}} + \frac{4 \cdot L_I \cdot C_{\mathcal{G}}}{\sqrt{|U_{micro}|}} \\
&\quad + \sqrt{\frac{2 \cdot \ln(4/\delta)}{|P_{micro}|}} + \sqrt{\frac{2 \cdot \ln(4/\delta)}{|U_{micro}|}} + p_{inc}(\mathcal{G}, g^*)
\end{aligned} \tag{29}$$

C Additional Experimental Results

C.1 Experiments with Low Imbalance Ratio

We present a comparative experiment on two long text datasets: IMDB and Amazon. The parameter σ_{micro} is set to [2, 3, 4, 5]. Due to space limitations in the main text, the additional experiments on the datasets Amazon are shown in table 6 in this appendix.

Table 4. The table presents the F1 scores of different algorithms under varying values of $\sigma_{micro} \in \{2, 3, 4, 5\}$, along with the estimated AUC with respect to changes in F1 on the IMDB Dataset.

Method	F1 Score				AUC_{F1}	
	2	3	4	5		
Macro	PN	77.73 ± 2.22	73.77 ± 0.92	63.98 ± 10.18	50.24 ± 22.06	66.43
	DeepSAD	52.22 ± 0.59	52.91 ± 1.37	54.84 ± 1.33	50.82 ± 1.21	52.70
MIL	ATT	82.27 ± 7.82	85.67 ± 1.41	78.78 ± 4.93	75.43 ± 2.50	80.54
	FGSA	81.50 ± 3.14	39.66 ± 36.71	52.30 ± 30.53	46.00 ± 39.91	54.87
PReNET		82.83 ± 2.11	77.07 ± 2.40	61.39 ± 9.70	65.83 ± 4.80	71.78
	DeepSAD	65.45 ± 3.58	62.67 ± 1.56	60.51 ± 1.16	59.78 ± 0.85	62.10
Micro	DeepSVDD	55.45 ± 1.36	55.99 ± 1.44	55.99 ± 0.60	55.14 ± 2.11	55.64
	uPU	80.95 ± 2.18	71.34 ± 2.77	74.05 ± 8.51	63.94 ± 6.10	72.57
nnPU	nnPU	86.15 ± 1.03	70.68 ± 2.85	66.67 ± 0.00	66.67 ± 0.00	72.54
	balancedPU	85.94 ± 1.78	79.12 ± 3.57	85.69 ± 0.93	80.93 ± 3.70	82.92
robustPU	robustPU	87.52 ± 0.53	86.24 ± 1.29	85.06 ± 0.79	77.80 ± 9.68	84.15
	BFGPU	88.12 ± 1.24	88.36 ± 0.58	86.57 ± 0.69	84.61 ± 0.43	86.92

It is evident that our proposed BFGPU achieves optimal performance in most settings. In only a few cases does the nnPU or robustPU loss function achieve optimal performance, but this also depends on our proposed ADT technique.

C.2 Experiments with High Imbalance Ratio

In addition to the SST-2 dataset, we conducted experiments on Sentiment140 which is a large short-text dataset with a focus on high imbalance ratios, setting σ_{micro} to [2, 4, 6, 8, 10].

Due to space limitations in the main text, the additional experiments on the Sentiment140 datasets are provided in table 7 in this appendix.

It is noticeable that when the imbalance ratio is high, the performance improvement brought by BFGPU is even greater compared to previous experiments. With larger values of σ_{micro} , we observed that many algorithms lack stability and may even fail. When algorithms fail, the evaluation metric F1 Score becomes highly unstable. This is because F1 Score does not treat positive and negative classes equally; more fundamentally, precision and recall are both centered around the

Table 5. The table presents the F1 scores of different algorithms under varying values of $\sigma_{\text{micro}} \in \{2, 4, 6, 8, 10\}$, along with the estimated AUC with respect to changes in F1 on the SST-2 Dataset.

Methods	F1 Score					AUC_{F1}	
	2	4	6	8	10		
Macro	PN	83.63 ± 0.21	79.35 ± 1.04	78.15 ± 2.81	75.77 ± 5.79	75.50 ± 3.23	78.48
	DeepSAD	75.24 ± 1.86	47.14 ± 13.51	28.13 ± 9.66	13.04 ± 9.22	7.00 ± 7.06	34.11
MIL	ATT	80.54 ± 0.51	62.39 ± 7.22	45.00 ± 36.50	0.00 ± 0.00	48.79 ± 30.96	47.34
	FGSA	49.38 ± 43.89	44.44 ± 38.49	66.67 ± 0.00	44.44 ± 38.49	44.44 ± 38.49	49.87
Micro	PReNET	73.67 ± 10.48	53.84 ± 7.58	48.68 ± 6.08	48.77 ± 16.00	36.10 ± 12.41	52.21
	DeepSAD	51.95 ± 12.30	14.95 ± 2.18	9.01 ± 7.18	9.92 ± 2.40	14.18 ± 4.29	20.00
Micro	DeepSVDD	24.98 ± 20.38	12.08 ± 5.99	26.98 ± 19.65	10.96 ± 1.51	13.30 ± 4.16	17.66
	uPU	76.82 ± 3.40	64.43 ± 6.62	62.13 ± 6.88	60.79 ± 10.15	67.56 ± 1.27	66.35
Micro	nnPU	84.00 ± 1.25	66.74 ± 0.10	66.67 ± 0.00	66.67 ± 0.00	66.67 ± 0.00	70.15
	balancedPU	80.75 ± 4.89	78.73 ± 6.27	52.51 ± 37.17	61.83 ± 7.17	70.48 ± 5.39	68.86
Micro	robustPU	86.31 ± 0.72	76.10 ± 6.57	74.79 ± 3.74	63.29 ± 10.26	62.90 ± 6.51	72.68
	BFGPU	88.73 ± 0.61	84.13 ± 0.30	83.96 ± 1.10	81.95 ± 1.87	84.41 ± 1.64	84.64

Table 6. The table presents AvgAcc and F1 scores of different algorithms under varying values of $\sigma_{\text{micro}} \in \{2, 3, 4, 5\}$, along with the estimated AUC with respect to changes in AvgAcc and F1 on the Amazon Dataset.

Method	AvgAcc				AUC_{AvgAcc}	
	2	3	4	5		
Macro	PN	89.11 ± 0.19	87.82 ± 0.23	84.74 ± 0.95	81.97 ± 0.60	85.91
	DeepSAD	85.55 ± 0.43	71.88 ± 6.80	63.31 ± 1.65	60.83 ± 3.43	70.39
MIL	ATT	87.96 ± 0.93	86.37 ± 1.23	85.60 ± 0.18	69.13 ± 15.83	82.27
	FGSA	59.46 ± 16.39	64.73 ± 14.45	52.50 ± 4.33	50.00 ± 0.00	56.67
Micro	PReNET	87.15 ± 0.68	84.00 ± 2.50	77.88 ± 2.86	79.40 ± 1.56	82.11
	DeepSAD	62.86 ± 9.94	52.14 ± 0.99	51.20 ± 2.28	50.84 ± 0.17	54.26
Micro	DeepSVDD	50.2 ± 1.36	51.19 ± 0.74	50.45 ± 1.06	50.44 ± 0.59	50.60
	uPU	82.48 ± 0.38	76.92 ± 2.66	74.15 ± 2.31	74.69 ± 0.18	77.06
Micro	nnPU	85.11 ± 1.40	74.02 ± 5.18	50.00 ± 0.00	50.00 ± 0.00	64.78
	balancedPU	80.59 ± 7.70	81.69 ± 5.52	80.84 ± 6.93	82.91 ± 8.14	81.51
Micro	robustPU	89.28 ± 0.52	87.07 ± 0.63	86.34 ± 0.34	82.47 ± 1.08	86.29
	BFGPU	89.87 ± 0.13	88.15 ± 0.97	86.71 ± 0.18	85.57 ± 0.67	87.58

Method	F1 Score				AUC_{F1}	
	2	3	4	5		
Macro	PN	89.10 ± 0.20	87.86 ± 0.26	84.73 ± 0.95	82.15 ± 0.51	85.96
	DeepSAD	88.22 ± 0.25	85.87 ± 0.15	83.02 ± 0.60	78.63 ± 0.93	83.94
MIL	ATT	88.24 ± 0.91	86.73 ± 1.33	86.16 ± 0.15	65.79 ± 19.75	81.73
	FGSA	47.01 ± 20.89	63.63 ± 14.12	10.08 ± 17.43	44.44 ± 38.49	41.29
Micro	PReNET	86.10 ± 0.88	81.97 ± 3.58	72.85 ± 4.66	75.66 ± 2.73	79.14
	DeepSAD	85.47 ± 0.54	72.34 ± 6.42	63.52 ± 1.48	59.47 ± 3.18	70.20
Micro	DeepSVDD	47.01 ± 40.89	63.63 ± 14.12	10.08 ± 17.43	44.44 ± 38.49	41.29
	uPU	79.82 ± 0.62	71.43 ± 4.48	67.49 ± 4.27	68.79 ± 3.65	71.88
Micro	nnPU	86.63 ± 1.09	79.34 ± 3.11	66.67 ± 0.00	66.67 ± 0.00	74.83
	balancedPU	78.50 ± 11.50	81.24 ± 6.09	81.38 ± 6.31	83.76 ± 0.71	81.22
Micro	robustPU	89.06 ± 0.71	86.60 ± 0.83	85.85 ± 0.70	82.18 ± 1.25	85.92
	BFGPU	90.03 ± 0.08	88.51 ± 1.05	87.44 ± 0.17	86.50 ± 0.40	88.12

positive class. Thus, the results in F1 Score can vary significantly depending on whether the classification leans towards
Manuscript submitted to ACM

Table 7. The table presents AvgAcc and F1 scores of different algorithms under varying values of $\sigma_{\text{micro}} \in \{2, 4, 6, 8, 10\}$, along with the estimated AUC with respect to changes in AvgAcc and F1 on the Sentiment140 Dataset.

Method		AvgAcc					AUC_{AvgAcc}
		2	4	6	8	10	
Macro	PN	74.37 \pm 0.40	69.80 \pm 0.37	66.81 \pm 0.48	65.09 \pm 0.19	62.20 \pm 0.48	67.65
	DeepSAD	57.03 \pm 4.17	53.41 \pm 0.94	52.56 \pm 1.24	51.37 \pm 0.63	51.21 \pm 0.99	53.12
MIL	ATT	71.27 \pm 0.36	64.97 \pm 3.24	52.88 \pm 4.98	50.06 \pm 0.10	50.16 \pm 0.28	57.87
	FGSA	64.17 \pm 3.13	53.46 \pm 4.03	50.00 \pm 0.00	50.00 \pm 0.00	50.00 \pm 0.00	53.53
	PreNET	70.41 \pm 3.74	57.11 \pm 7.11	55.56 \pm 4.83	54.85 \pm 2.93	50.00 \pm 0.00	57.59
Micro	DeepSAD	51.07 \pm 2.14	51.80 \pm 2.05	65.23 \pm 2.04	63.99 \pm 8.28	58.81 \pm 8.64	58.18
	DeepSVDD	49.65 \pm 0.55	50.09 \pm 0.18	49.70 \pm 0.58	49.83 \pm 0.72	50.27 \pm 0.29	49.91
	uPU	68.81 \pm 1.02	62.73 \pm 2.48	61.23 \pm 3.25	57.54 \pm 5.37	54.31 \pm 3.33	60.92
	nnPU	69.66 \pm 1.01	50.00 \pm 0.00	50.00 \pm 0.00	50.00 \pm 0.00	50.00 \pm 0.00	53.93
	balancedPU	72.55 \pm 2.23	70.26 \pm 0.16	66.16 \pm 1.53	50.00 \pm 0.00	50.68 \pm 0.54	61.93
	robustPU	74.65 \pm 0.70	70.13 \pm 1.63	66.94 \pm 0.40	59.14 \pm 8.58	62.88 \pm 0.27	66.74
	BFGPU	75.86 \pm 1.01	70.68 \pm 0.97	67.95 \pm 1.53	66.34 \pm 1.25	64.45 \pm 0.35	69.06
	F1 Score						AUC_{F1}
Method		2	4	6	8	10	AUC_{F1}
		73.99 \pm 0.72	68.75 \pm 0.44	64.94 \pm 1.66	63.86 \pm 0.52	59.50 \pm 1.48	66.21
Macro	DeepSAD	57.24 \pm 4.26	53.61 \pm 1.16	52.03 \pm 1.33	51.55 \pm 0.71	51.83 \pm 0.77	53.25
	ATT	67.64 \pm 0.52	56.56 \pm 5.58	37.40 \pm 34.07	22.85 \pm 37.96	23.34 \pm 37.56	41.56
MIL	FGSA	52.19 \pm 8.97	16.28 \pm 17.59	44.44 \pm 38.49	44.44 \pm 38.49	44.44 \pm 38.49	40.36
	PreNET	63.36 \pm 8.65	26.89 \pm 24.61	44.62 \pm 19.17	20.65 \pm 12.24	66.67 \pm 0.00	44.44
	DeepSAD	54.65 \pm 1.80	55.89 \pm 1.76	67.50 \pm 1.80	66.55 \pm 7.42	61.86 \pm 7.61	61.29
Micro	DeepSVDD	53.33 \pm 0.67	54.27 \pm 0.20	53.37 \pm 0.71	53.61 \pm 1.05	54.11 \pm 0.49	53.74
	uPU	60.88 \pm 2.42	57.32 \pm 10.29	48.65 \pm 13.84	60.66 \pm 4.54	66.66 \pm 0.21	58.83
	nnPU	75.50 \pm 0.56	66.67 \pm 0.00	66.67 \pm 0.00	66.67 \pm 0.00	66.67 \pm 0.00	68.44
	balancedPU	72.00 \pm 1.80	69.98 \pm 0.95	70.80 \pm 0.84	44.44 \pm 31.43	66.83 \pm 0.24	64.81
	robustPU	73.43 \pm 1.05	67.66 \pm 1.83	61.80 \pm 2.36	64.00 \pm 2.35	55.89 \pm 0.48	64.55
	BFGPU	77.21 \pm 0.73	73.27 \pm 0.95	69.80 \pm 3.18	67.21 \pm 2.94	66.40 \pm 0.68	70.78

the positive or negative class to the same extent. In contrast, the metric of average accuracy possesses greater stability and fairness.

C.3 Experiments with Imbalance at Both Macro and Micro Levels

On the SST-2 dataset, we set σ_{macro} to 5 and explored how algorithm performance varied with σ_{micro} set to [2, 4, 6, 8, 10].

Due to space limitations in the main text, the experimental statistical data on the SST-2 dataset are provided in table 8 in this appendix.

In settings where both imbalances coexist, with the total proportion of negative information in the text dataset reaching its extreme low, we found that most comparative methods failed. However, BFGPU still maintained stable and excellent performance in this extreme scenario, demonstrating its strong versatility.

C.4 Ablation Study

To explore the necessity of each component of BFGPU, we conducted ablation experiments, comparing the algorithm's performance without the new loss function, without pseudo-labeling, and without the threshold adjustment technique. We

Table 8. Experimental Results on the SST-2 Dataset with Imbalance at Both Macro and Micro Levels.

Method	AvgAcc					AUC_{AvgAcc}	
	2	4	6	8	10		
Macro	PN	72.65 ± 2.15	70.46 ± 4.82	69.32 ± 1.90	63.52 ± 6.64	55.42 ± 3.59	66.27
	DeepSAD	51.93 ± 1.63	54.79 ± 2.63	52.17 ± 1.77	45.91 ± 2.71	49.22 ± 1.98	50.80
MIL	ATT	77.90 ± 2.91	71.29 ± 14.46	51.21 ± 1.51	56.29 ± 7.21	58.14 ± 14.10	62.96
	FGSA	50.00 ± 0.00	50.00				
Micro	PReNET	50.00 ± 0.00	50.00				
	DeepSAD	50.37 ± 2.14	53.13 ± 2.07	49.52 ± 2.80	45.60 ± 3.80	50.39 ± 3.95	49.80
Micro	DeepSVDD	51.38 ± 1.99	54.29 ± 2.23	50.00 ± 6.32	48.74 ± 3.93	53.10 ± 6.40	51.50
	uPU	71.45 ± 15.17	77.89 ± 1.23	57.25 ± 7.49	50.00 ± 0.00	50.00 ± 0.00	61.32
Micro	nnPU	50.00 ± 0.00	50.00				
	balancedPU	54.24 ± 7.34	50.00 ± 0.00	50.00 ± 0.00	50.00 ± 0.00	50.00 ± 0.00	50.85
Micro	robustPU	75.60 ± 5.76	76.57 ± 2.73	58.21 ± 14.22	50.00 ± 0.00	50.00 ± 0.00	62.08
	BFGPU	80.48 ± 3.23	78.22 ± 2.48	73.19 ± 4.41	63.84 ± 11.18	67.83 ± 0.46	72.71
Method	F1 Score					AUC_{F1}	
	2	4	6	8	10		
Macro	PN	78.16 ± 1.37	76.95 ± 2.89	75.92 ± 1.08	72.56 ± 3.22	68.00 ± 1.67	74.32
	DeepSAD	56.88 ± 3.37	59.33 ± 5.46	44.46 ± 6.05	36.40 ± 14.12	23.49 ± 14.07	44.11
MIL	ATT	81.46 ± 1.93	77.75 ± 8.28	67.21 ± 0.68	69.70 ± 3.55	70.73 ± 7.03	73.37
	FGSA	66.67 ± 0.00	66.67				
Micro	PReNET	66.67 ± 0.00	66.67				
	DeepSAD	47.48 ± 3.96	51.85 ± 1.29	44.26 ± 3.04	38.50 ± 2.66	47.01 ± 5.18	45.82
Micro	DeepSVDD	48.99 ± 4.43	51.81 ± 2.14	44.85 ± 6.23	48.33 ± 11.22	50.36 ± 4.26	48.87
	uPU	77.09 ± 7.37	78.81 ± 0.83	68.25 ± 2.24	66.67 ± 0.00	66.67 ± 0.00	71.50
Micro	nnPU	66.67 ± 0.00	66.67				
	balancedPU	13.85 ± 23.99	0.00 ± 0.00	0.00 ± 0.00	0.00 ± 0.00	0.00 ± 0.00	2.77
Micro	robustPU	80.07 ± 3.93	80.74 ± 1.57	71.03 ± 7.56	66.67 ± 0.00	66.67 ± 0.00	73.04
	BFGPU	83.48 ± 2.32	81.59 ± 1.29	78.76 ± 2.76	64.92 ± 18.60	74.24 ± 3.95	76.60

Table 9. The table presents AvgAcc and F1 results of the ablation study under varying values of $\sigma_{micro} \in \{2, 3, 4, 5\}$ on the IMDB dataset.

PU Loss	Pseudo Labels	Threshold	AvgAcc			
			2	3	4	5
×	✓	✓	84.98 ± 3.14	84.27 ± 2.12	85.55 ± 0.31	62.19 ± 10.22
✓	✗	✓	88.13 ± 0.76	86.04 ± 0.66	85.40 ± 0.18	83.02 ± 1.35
✓	✓	✗	88.25 ± 0.90	86.97 ± 0.89	85.40 ± 0.18	81.18 ± 2.13
✓	✓	✓	88.13 ± 1.07	87.93 ± 0.58	86.02 ± 0.69	83.64 ± 0.78
PU Loss	Pseudo Labels	Threshold	F1 Score			
			2	3	4	5
×	✓	✓	82.34 ± 2.83	84.06 ± 2.37	85.67 ± 0.43	58.35 ± 13.32
✓	✗	✓	88.63 ± 0.55	86.95 ± 0.42	85.01 ± 0.88	84.36 ± 0.74
✓	✓	✗	88.44 ± 0.97	86.50 ± 1.12	85.01 ± 0.88	78.92 ± 3.39
✓	✓	✓	88.12 ± 1.24	88.36 ± 0.58	86.57 ± 0.69	84.61 ± 0.43

performed these experiments on the IMDB and SST-2 datasets, setting σ_{micro} to $[2, 4, 6, 8, 10]$. Due to space limitations in the main text, the additional experiments on the SST-2 dataset are provided in table 10 in this appendix.

The experimental results indicate that each component of BFGPU is crucial, collectively ensuring the algorithm's stability and excellent performance.

Table 10. The table presents AvgAcc and F1 results of the ablation study under varying values of $\sigma_{micro} \in \{2, 3, 4, 5\}$ on the SST-2 dataset.

PU Loss	Pseudo Labels	Threshold	AvgAcc				
			2	4	6	8	10
✗	✓	✓	85.27 \pm 1.50	83.33 \pm 0.84	79.95 \pm 2.46	77.36 \pm 2.67	79.07 \pm 3.80
✓	✗	✓	87.75 \pm 2.08	86.14 \pm 1.07	71.50 \pm 14.69	66.35 \pm 12.76	80.62 \pm 3.33
✓	✓	✗	86.83 \pm 0.13	72.11 \pm 12.07	74.15 \pm 1.49	58.81 \pm 5.78	60.85 \pm 7.91
✓	✓	✓	88.40 \pm 0.68	82.51 \pm 0.62	82.13 \pm 0.90	79.56 \pm 1.60	82.56 \pm 1.64

PU Loss	Pseudo Labels	Threshold	F1 Score				
			2	4	6	8	10
✗	✓	✓	86.65 \pm 0.92	84.95 \pm 0.64	82.74 \pm 1.33	80.87 \pm 2.12	81.32 \pm 2.96
✓	✗	✓	88.41 \pm 1.80	87.31 \pm 0.95	61.39 \pm 31.32	51.26 \pm 36.66	82.65 \pm 2.92
✓	✓	✗	86.88 \pm 0.54	71.80 \pm 10.90	68.84 \pm 2.64	40.53 \pm 8.76	57.33 \pm 12.78
✓	✓	✓	88.73 \pm 0.61	84.13 \pm 0.30	83.96 \pm 1.10	81.95 \pm 1.87	84.41 \pm 1.64

Table 11. This table presents the AvgAcc of the sensitive analysis of λ_{bfgpu} on the SST-2 dataset.

λ_{bfgpu}	1	2	3	4	5
AvgAcc	83.41	84.72	84.99	84.55	82.79
F1Score	84.56	85.68	85.83	85.56	84.45

Table 12. This table presents the AvgAcc of the sensitive analysis of λ_{pse} on the SST-2 dataset.

λ_{pse}	1	2	3	4	5
AvgAcc	83.41	84.29	84.68	84.64	84.94
F1Score	84.56	85.23	85.49	85.51	85.67

C.5 Sensitive Analysis

We have supplemented the sensitivity analysis of hyperparameters λ_{bfgpu} and λ_{pse} . We completed experiments on the IMDB dataset, setting $\sigma_{micro} = 5$. We set the variation range of the two parameters to $[1, 2, 3, 4, 5]$, and kept one constant while varying the other. Due to space limitations in the main text, the sensitive analysis of λ_{pse} on the SST-2 dataset are provided in table 12 in this appendix.

Experiments have demonstrated that the performance of the algorithm remains relatively stable under different hyperparameter settings, so there is no need to worry too much about hyperparameter tuning.